

Matrix completion based on Gaussian parameterized belief propagation

Koki Okajima and Yoshiyuki Kabashima

Graduate School of Science, The University of Tokyo, Bunkyo, Tokyo 113-0033, Japan

Abstract. We develop a message-passing algorithm for noisy matrix completion problems based on matrix factorization. The algorithm is derived by approximating message distributions of belief propagation with Gaussian distributions that share the same first and second moments. We also derive a memory-friendly version of the proposed algorithm by applying a perturbation treatment commonly used in the literature of approximate message passing. In addition, a damping technique, which is demonstrated to be crucial for optimal performance, is introduced without computational strain, and the relationship to the message-passing version of alternating least squares, a method reported to be optimal in certain settings, is discussed. Experiments on synthetic datasets show that while the proposed algorithm quantitatively exhibits almost the same performance under settings where the earlier algorithm is optimal, it is advantageous when the observed datasets are corrupted by non-Gaussian noise. Experiments on real-world datasets also emphasize the performance differences between the two algorithms.

Keywords: matrix completion, matrix factorization, belief propagation

1. Introduction

Estimating the elements of a matrix from its sparse, noisy observation is a widely studied problem relevant to real-world applications such as collaborative filtering and recommender systems. Although this problem is ill-defined, manageable results can still be obtained by constraining the observed matrix to be of low rank.

A primary setting for noisy low-rank matrix completion would be to minimize the rank of the matrix subject to constraining the observed and estimated entries by a margin δ :

$$\min_{X \in \mathbb{R}^{N \times M}} \text{rank } X \quad \text{subject to} \quad |x_{ij} - y_{ij}| \leq \delta, \quad (i, j) \in \Omega, \quad (1)$$

where $X = \{x_{ij}\}$ and Ω denotes the set of subscripts (i, j) of the observed elements y_{ij} , $1 \leq i \leq N$, $1 \leq j \leq M$. Unfortunately, accurately solving this problem is computationally difficult. One approach for practically overcoming this difficulty is to convert (1) into a convex problem, which is solvable via semidefinite programming in a practical time scale by substituting the rank function with the nuclear norm [1, 2]. Surprisingly, this heuristic approach is known to fully recover the matrix itself under particular assumptions [2–4], making this treatment favorable for both practical use and theoretical analysis. Nevertheless, semidefinite programming that handles the full matrix explicitly encounters high computational costs in

terms of both time and space complexity.

One way to resolve this difficulty is to factorize the objective matrix, i.e., $X = UV^T$, and estimate the factor matrices U, V . Although this makes the problem non-convex, its global minimum is known to coincide with the optimal solution when U and V have rank higher than the true rank. Its desirable scalability, and the fact that all local minima equivalently minimize the nuclear norm given sufficient numbers of observations [5] make this formulation appealing for solving the matrix completion problem.

Owing to the sparse nature of the problem, belief propagation (BP), or more commonly known as the cavity method in statistical physics, is an efficient method for finding the solution. The earliest application of BP-based algorithms to matrix completion is the message-passing version of alternating least squares (ALS-MP) [6], which was rediscovered by [7] as edge least squares. In a synthetic and noisy setup, the root-mean-squared error (RMSE) of the estimated matrix using ALS-MP was empirically demonstrated to be near an oracle bound. More recently, a cavity-based approach was proposed [8], which had significantly lower time and space complexity, but required more observed entries compared with ALS-MP. More precisely, [8] demonstrated that the algorithm is as computationally efficient as the original version of alternating least squares [7, 9], which is, however, outperformed by ALS-MP in terms of achieved performance.

This study aims to develop another BP-based algorithm, which has the same time and space complexity as ALS-MP. The proposed method seeks to approximate message distributions of BP by Gaussians with moment matching imposed up to its second order, which is analogous to the scheme used in expectation propagation (EP) [10]. Although the performance of our method is similar to that of ALS-MP under synthetic settings, experimental results show that our method is more robust in situations where the set of observed data is corrupted by non-Gaussian noise. Besides, we demonstrate that damping is necessary for the two algorithms to achieve optimal performance. This is confirmed by a comparison with the results from population dynamics (PD), which simulates the behavior of the message-passing algorithms in the large system limit. Approximate versions for both BP methods are also provided to reduce the necessary space complexity. Applications to real-world datasets indicate that our method outperforms conventional approaches.

The outline of this paper is as follows. In Section 2, we derive the BP-based algorithm and its memory-friendly version. In addition, we rederive ALS-MP in analog to our derivation. Comparisons between the two methods on an algorithmic level are also provided. Subsection 2.4 is devoted to explaining the PD algorithm, which is used to provide a crucial baseline for performance achievable in the large system limit. The algorithm's performance via numerical experiments on synthetic and real datasets is presented in sections 3 and 4, respectively. Finally, Section 5 summarizes this work and highlights possible future research directions.

2. The Algorithms

By convex relaxation, (1) is converted to the minimization of the nuclear norm as

$$\min_{X \in \mathbb{R}^{N \times M}} \|X\|_* \quad \text{subject to} \quad |x_{ij} - y_{ij}| \leq \delta, \quad (i, j) \in \Omega, \quad (2)$$

where $\|X\|_*$ is the nuclear norm of matrix X , which is given by the sum of its singular values. Although this is readily solvable in polynomial time complexity via semidefinite programming, we employ the equality [11]

$$\|X\|_* = \frac{1}{2} \min_{\substack{U \in \mathbb{R}^{N \times R}, V \in \mathbb{R}^{M \times R}, \\ UV^T = X}} \|U\|_F^2 + \|V\|_F^2, \quad (3)$$

for $R \geq \text{rank } X$ to further reduce its computational complexity. Here, $\|\cdot\|_F$ denotes the Frobenius norm of the matrix. The Lagrangian dual of (2) using (3) is given by the following equation, where λ is a function of δ :

$$\min_{U \in \mathbb{R}^{N \times R}, V \in \mathbb{R}^{M \times R}} \frac{1}{2} \sum_{(i,j) \in \Omega} (y_{ij} - \mathbf{u}_i^T \mathbf{v}_j)^2 + \frac{\lambda}{2} \sum_{i=1}^N \|\mathbf{u}_i\|^2 + \frac{\lambda}{2} \sum_{j=1}^M \|\mathbf{v}_j\|^2. \quad (4)$$

Typically, λ is a parameter controlling the strength of the nuclear norm regularization. Our introduction of λ motivates us to tune this parameter to satisfy the constraint of (2). However, the optimal value of δ , and consequently λ , which offers the best performance is unknown in advance under most situations. In such cases, the parameter is to be determined using hyperparameter tuning techniques such as cross validation for best results.

This optimization problem with respect to $N + M$ R -dimensional vectors $U = (\mathbf{u}_1, \dots, \mathbf{u}_N)^T$, $V = (\mathbf{v}_1, \dots, \mathbf{v}_M)^T$ is reduced to the dual form of (2), which is $\min \sum_{(i,j) \in \Omega} (y_{ij} - x_{ij})^2 + \lambda \|X\|_*$, if R is larger than or equal to the rank of the optimal solution X . Throughout this paper, we focus on this factorized formulation.

In other words, the solution is given by maximizing the posterior distribution that is composed of likelihood

$$p(y_{ij} | \mathbf{u}_i, \mathbf{v}_j) \propto \exp \left[-\frac{\beta}{2} (y_{ij} - \mathbf{u}_i^T \mathbf{v}_j)^2 \right], \quad (i, j) \in \Omega, \quad (5)$$

which implies that the observations are assumed to be corrupted by Gaussian noise with variance β^{-1} , and a Gaussian prior distribution that is dependent on the noise intensity:

$$p(\mathbf{u}_i) \propto \exp \left(-\frac{\beta\lambda}{2} \|\mathbf{u}_i\|^2 \right), \quad p(\mathbf{v}_j) \propto \exp \left(-\frac{\beta\lambda}{2} \|\mathbf{v}_j\|^2 \right), \quad 1 \leq i \leq N, \quad 1 \leq j \leq M. \quad (6)$$

2.1. Derivation of the Gaussian BP algorithm

The proposed BP algorithm aims at approximating the posterior distribution given by (5) and (6). For this, we first express the variable dependence of the posterior on a factor graph (figure 1). Here, each interacting factor represents the likelihood for a single observed

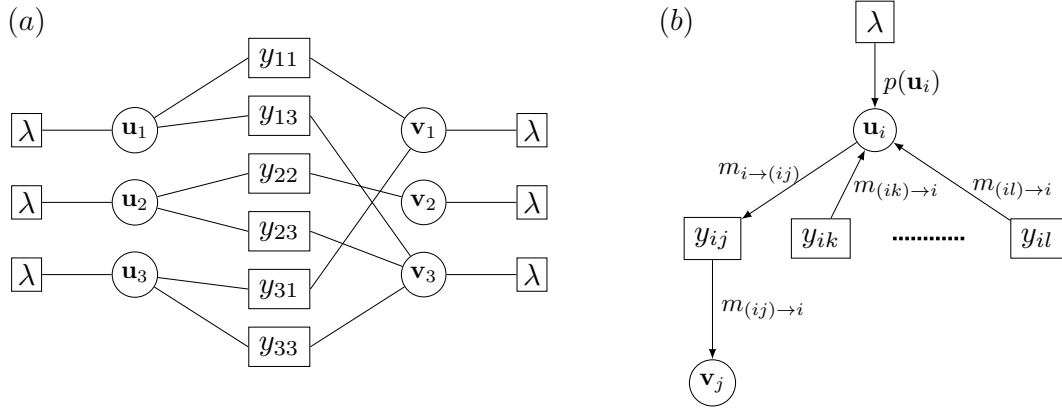


Figure 1. (a) An example of a factor graph for $N = M = 3$ and six observations. (b) Illustration of the message-passing algorithm on a factor graph. Node i collects the prior message and the messages from $(ik), \dots, (il)$, and passes $m_{i \rightarrow (ij)}$ to factor (ij) . As a result, factor (ij) passes message $m_{(ij) \rightarrow j}$ to node j . Irrelevant nodes and factors are not shown for ease of visualization.

variable, $p(y_{ij}|\mathbf{u}_i, \mathbf{v}_j)$, and is indexed by the pair of indices (i, j) . Without causing confusion, we denote the factors using the Greek letters μ, ν, \dots without explicitly writing the pair of indices. The prior factors, illustrated by the boxed λ , are individually connected to each variable node.

The BP algorithm is an iterative procedure to find the fixed point solution of the following closed equations for the distributions defined on the edges of the factor graph:

$$m_{\mu \rightarrow i}^{t+1}(\mathbf{u}_i) \propto \int d\mathbf{v}_j p(y_{ij}|\mathbf{u}_i, \mathbf{v}_j) m_{j \rightarrow \mu}^t(\mathbf{v}_j), \quad (7a)$$

$$m_{i \rightarrow \mu}^{t+1}(\mathbf{u}_i) \propto p(\mathbf{u}_i) \prod_{\nu \in \partial i \setminus \mu} m_{\nu \rightarrow i}^{t+1}(\mathbf{u}_i), \quad (7b)$$

$$m_{\mu \rightarrow j}^{t+1}(\mathbf{v}_j) \propto \int d\mathbf{u}_i p(y_{ij}|\mathbf{u}_i, \mathbf{v}_j) m_{i \rightarrow \mu}^{t+1}(\mathbf{u}_i), \quad (7c)$$

$$m_{j \rightarrow \mu}^{t+1}(\mathbf{v}_j) \propto p(\mathbf{v}_j) \prod_{\nu \in \partial j \setminus \mu} m_{\nu \rightarrow j}^{t+1}(\mathbf{v}_j). \quad (7d)$$

The expression ∂i denotes the set of factors connected to node i , whereas the superscript $t = 0, 1, \dots$ denotes the iteration number. The function $m_{\mu \rightarrow i}^t(\mathbf{u}_i)$ represents the marginal likelihood (or cavity bias) of \mathbf{u}_i , given by y_{ij} , whereas $m_{i \rightarrow \mu}^t(\mathbf{u}_i)$ is the marginal distribution of \mathbf{u}_i in the absence of factor y_{ij} (or the cavity distribution). The approximated posterior distributions of the nodes at iteration t are given by

$$p(\mathbf{u}_i|Y) \propto p(\mathbf{u}_i) \prod_{\mu \in \partial i} m_{\mu \rightarrow i}^t(\mathbf{u}_i), \quad (8)$$

$$p(\mathbf{v}_j|Y) \propto p(\mathbf{v}_j) \prod_{\mu \in \partial j} m_{\mu \rightarrow j}^t(\mathbf{v}_j). \quad (9)$$

Solving (7a)–(7d) accurately is difficult, as these are functional equations with continuous degrees of freedom. Therefore, we approximately handle the BP equations using a few parameters. More explicitly, we parameterize the message distributions by those of the

general R -dimensional Gaussian forms as

$$m_{i \rightarrow \mu}^t(\mathbf{u}_i) \propto \exp \left[-\frac{\beta}{2} \mathbf{u}_i^\top A_{i \rightarrow \mu}(t) \mathbf{u}_i + \beta \mathbf{B}_{i \rightarrow \mu}^\top(t) \mathbf{u}_i \right], \quad (10a)$$

$$m_{j \rightarrow \mu}^t(\mathbf{v}_j) \propto \exp \left[-\frac{\beta}{2} \mathbf{v}_j^\top C_{j \rightarrow \mu}(t) \mathbf{v}_j + \beta \mathbf{D}_{j \rightarrow \mu}^\top(t) \mathbf{v}_j \right], \quad (10b)$$

where $A_{i \rightarrow \mu}, C_{j \rightarrow \mu} \in \mathbb{R}^{R \times R}$ and $\mathbf{B}_{i \rightarrow \mu}, \mathbf{D}_{j \rightarrow \mu} \in \mathbb{R}^R$ denote the natural parameters.

For brevity, we hereafter omit the iteration number unless otherwise needed. Inserting (10b) into the right-hand side of (7a), we obtain the marginal likelihood as (a detailed derivation is given in the Appendix)

$$\int d\mathbf{v}_j p(y_{ij} | \mathbf{u}_i, \mathbf{v}_j) m_{j \rightarrow \mu}(\mathbf{v}_j) \propto (1 + \mathbf{u}_i^\top C_{j \rightarrow \mu}^{-1} \mathbf{u}_i)^{-1/2} \exp \left[-\frac{\beta}{2} \frac{(y_{ij} - \mathbf{u}_i^\top C_{j \rightarrow \mu}^{-1} \mathbf{D}_{j \rightarrow \mu})^2}{1 + \mathbf{u}_i^\top C_{j \rightarrow \mu}^{-1} \mathbf{u}_i} \right]. \quad (11)$$

Note that if $|\partial j|$ is sufficiently larger than R , the Gaussian parameterization is asymptotically exact. This is because the eigenvalue of matrix $C_{j \rightarrow \mu}$ typically scales with $|\partial j|$ (see (7d)), and thus $\mathbf{u}_i^\top C_{j \rightarrow \mu}^{-1} \mathbf{u}_i$ can be ignored. This does not necessarily imply that $|\partial j|$ must be $O(N)$, and observations can be sparse, e.g. $|\partial j| = O(\log N)$ for $R = O(1)$. The corresponding algorithm which applies this approximation is indeed ALS-MP, which is introduced in 2.3. Otherwise, (11) is not of Gaussian form with respect to \mathbf{u}_i , and does not lead to a closed set of equations. To close the update equations for the parameters of A , \mathbf{B} , C , and \mathbf{D} in the limit of $\beta \rightarrow \infty$, we resort to the moment matching condition up to second order similarly as employed in [10].

For this, we introduce the partition function based on (11) as

$$Z(\theta) = \int d\mathbf{u} (1 + \mathbf{u}^\top C^{-1} \mathbf{u})^{-1/2} \exp \left[-\frac{\beta}{2} \frac{(y_{ij} - \mathbf{u}^\top C^{-1} \mathbf{D})^2}{1 + \mathbf{u}^\top C^{-1} \mathbf{u}} + \beta \theta^\top \mathbf{u} - \frac{\beta \epsilon}{2} \|\mathbf{u}\|^2 \right], \quad (12)$$

where we dropped all indices for notational simplicity and used a Gaussian factor $\exp(-\beta \epsilon \|\mathbf{u}\|^2 / 2)$, $0 < \epsilon \ll 1$, to prevent the integral from diverging. For $\beta \gg 1$, evaluating the right-hand side of (12) using the Laplace approximation yields an expression

$$\frac{1}{\beta} \log Z(\theta) = \max_{\mathbf{u}} \left[-\frac{1}{2} \frac{(y_{ij} - \mathbf{u}^\top C^{-1} \mathbf{D})^2}{1 + \mathbf{u}^\top C^{-1} \mathbf{u}} + \theta^\top \mathbf{u} - \frac{\epsilon}{2} \|\mathbf{u}\|^2 \right], \quad (13)$$

which offers the maximum condition as

$$\frac{y - \mathbf{u}^\top \mathbf{v}^*}{1 + \mathbf{u}^\top C^{-1} \mathbf{u}} \mathbf{v}^* + \left(\frac{y - \mathbf{u}^\top \mathbf{v}^*}{1 + \mathbf{u}^\top C^{-1} \mathbf{u}} \right)^2 C^{-1} \mathbf{u} + \theta - \epsilon \mathbf{u} = \mathbf{0}, \quad (14)$$

where $\mathbf{v}^* = C^{-1} \mathbf{D}$. For $\|\theta\| \ll 1$ and $\epsilon \ll 1$, the solution to this equation is given by

$$\mathbf{u}^*(\theta) = \frac{y}{\|\mathbf{v}^*\|^2} \mathbf{v}^* + \left[\epsilon \mathbf{1}_R + \frac{\mathbf{v}^*(\mathbf{v}^*)^\top}{1 + y^2 \alpha} \right]^{-1} \theta + O(\|\theta\|^2, \epsilon), \quad (15)$$

where $\alpha \equiv (\mathbf{v}^*)^\top C^{-1} \mathbf{v}^* / \|\mathbf{v}^*\|^4$. This means that the first and second moments of the distribution derived by normalizing (11) are provided as

$$\langle \mathbf{u} \rangle = \frac{1}{\beta} \frac{\partial}{\partial \theta} \log Z(\theta) \Big|_{\theta=0} = \mathbf{u}^*(\theta) \Big|_{\theta=0} = \frac{y}{\|\mathbf{v}^*\|^2} \mathbf{v}^* + O(\epsilon) \quad (16)$$

and

$$\langle \mathbf{u}\mathbf{u}^\top \rangle - \langle \mathbf{u} \rangle \langle \mathbf{u} \rangle^\top = \frac{1}{\beta^2} \frac{\partial^2}{\partial \boldsymbol{\theta} \partial \boldsymbol{\theta}} \log Z(\boldsymbol{\theta}) \Big|_{\boldsymbol{\theta}=\mathbf{0}} = \frac{1}{\beta} \frac{\partial \mathbf{u}^*(\boldsymbol{\theta})}{\partial \boldsymbol{\theta}} \Big|_{\boldsymbol{\theta}=\mathbf{0}} = \frac{1}{\beta} \left[\boldsymbol{\epsilon} \mathbf{1}_R + \frac{\mathbf{v}^*(\mathbf{v}^*)^\top}{1 + y^2 \alpha} \right]^{-1} + o(\beta^{-1}), \quad (17)$$

respectively, where $\mathbf{1}_R \in \mathbb{R}^{R \times R}$ is the identity matrix. Approximating the right-hand side of (7a) using a Gaussian function that reproduces these moments, which corresponds to the moment matching condition, and recovering the relevant indices results in

$$m_{\mu \rightarrow i}(\mathbf{u}) \propto \exp \left(-\frac{\beta}{2} \frac{\mathbf{u}^\top \mathbf{v}_{j \rightarrow \mu} \mathbf{v}_{j \rightarrow \mu}^\top \mathbf{u}}{1 + y_{ij}^2 \alpha_{j \rightarrow \mu}} + \beta \frac{y_{ij} \mathbf{v}_{j \rightarrow \mu}^\top \mathbf{u}}{1 + y_{ij}^2 \alpha_{j \rightarrow \mu}} \right), \quad (18)$$

under the limit $\epsilon \rightarrow +0$, where $\mathbf{v}_{j \rightarrow \mu} \equiv C_{j \rightarrow \mu}^{-1} \mathbf{D}_{j \rightarrow \mu}$ and $\alpha_{j \rightarrow \mu} \equiv \mathbf{v}_{j \rightarrow \mu}^\top C_{j \rightarrow \mu}^{-1} \mathbf{v}_{j \rightarrow \mu} / \|\mathbf{v}_{j \rightarrow \mu}\|^4$. Inserting this expression into (7b) provides update rules for \mathbf{A} and \mathbf{B} as

$$\mathbf{A}_{i \rightarrow \mu} = \lambda \mathbf{1}_R + \sum_{v \in \partial i \setminus \mu} \frac{\mathbf{v}_{j \rightarrow v} \mathbf{v}_{j \rightarrow v}^\top}{1 + y_{ij}^2 \alpha_{j \rightarrow v}}, \quad (19)$$

$$\mathbf{B}_{i \rightarrow \mu} = \sum_{v \in \partial i \setminus \mu} \frac{y_{ij} \mathbf{v}_{j \rightarrow v}}{1 + y_{ij}^2 \alpha_{j \rightarrow v}}. \quad (20)$$

Similarly, the update rules for \mathbf{C} and \mathbf{D} are obtained as follows:

$$\mathbf{C}_{j \rightarrow \mu} = \lambda \mathbf{1}_R + \sum_{v \in \partial j \setminus \mu} \frac{\mathbf{u}_{i \rightarrow v} \mathbf{u}_{i \rightarrow v}^\top}{1 + y_{ij}^2 \alpha_{i \rightarrow v}}, \quad (21)$$

$$\mathbf{D}_{j \rightarrow \mu} = \sum_{v \in \partial j \setminus \mu} \frac{y_{ij} \mathbf{u}_{i \rightarrow v}}{1 + y_{ij}^2 \alpha_{i \rightarrow v}}, \quad (22)$$

where $\mathbf{u}_{i \rightarrow \mu} \equiv A_{i \rightarrow \mu}^{-1} \mathbf{B}_{i \rightarrow \mu}$ and $\alpha_{i \rightarrow \mu} \equiv \mathbf{u}_{i \rightarrow \mu}^\top A_{i \rightarrow \mu}^{-1} \mathbf{u}_{i \rightarrow \mu} / \|\mathbf{u}_{i \rightarrow \mu}\|^4$. The posterior distributions (8) and (9) are also given in Gaussian form as

$$p(\mathbf{u}_i | Y) \propto \exp \left(-\frac{\beta}{2} \mathbf{u}_i^\top A_i \mathbf{u}_i + \beta \mathbf{B}_i^\top \mathbf{u}_i \right), \quad (23)$$

$$A_i \equiv \lambda \mathbf{1}_R + \sum_{\mu \in \partial i} \frac{\mathbf{v}_{j \rightarrow \mu} \mathbf{v}_{j \rightarrow \mu}^\top}{1 + y_{ij}^2 \alpha_{j \rightarrow \mu}}, \quad \mathbf{B}_i \equiv \sum_{\mu \in \partial i} \frac{y_{ij} \mathbf{v}_{j \rightarrow \mu}}{1 + y_{ij}^2 \alpha_{j \rightarrow \mu}}, \quad (24)$$

and

$$p(\mathbf{v}_j | Y) \propto \exp \left(-\frac{\beta}{2} \mathbf{v}_j^\top C_j \mathbf{v}_j + \beta \mathbf{D}_j^\top \mathbf{v}_j \right), \quad (25)$$

$$C_j \equiv \lambda \mathbf{1}_R + \sum_{\mu \in \partial j} \frac{\mathbf{u}_{i \rightarrow \mu} \mathbf{u}_{i \rightarrow \mu}^\top}{1 + y_{ij}^2 \alpha_{i \rightarrow \mu}}, \quad \mathbf{D}_j \equiv \sum_{\mu \in \partial j} \frac{y_{ij} \mathbf{u}_{i \rightarrow \mu}}{1 + y_{ij}^2 \alpha_{i \rightarrow \mu}}. \quad (26)$$

Three issues are noteworthy here. First, the derived algorithm is analogous to EP [10] in terms of requiring the Gaussians to yield the same first and second moments. However, unlike our algorithm, EP employs the moment matching condition for the joint distribution

$$p(\mathbf{u}_i, \mathbf{v}_j) \propto p(y_{ij} | \mathbf{u}_i, \mathbf{v}_j) m_{i \rightarrow \mu}(\mathbf{u}_i) m_{j \rightarrow \mu}(\mathbf{v}_j),$$

which, in the limit of $\beta \rightarrow \infty$, is reduced to a set of coupled nonlinear equations with respect to the moments of \mathbf{u}_i and \mathbf{v}_j . Consequently, one cannot obtain closed forms of the update rules such as (18)–(24), which reduces the practicality of the algorithm. In contrast, our algorithm eliminates this difficulty by imposing the moment matching requirement on the cavity distributions (7a) and (7c). The second issue is regarding the computational cost. Although the algorithm involves the inverse of the matrix $A_{i \rightarrow \mu}$ and $C_{j \rightarrow \mu}$, these can be calculated explicitly using the Sherman–Morrison formula in $O(R^2)$ time complexity during the iterations once $A_{i \rightarrow \mu}^{-1}$ and $C_{j \rightarrow \mu}^{-1}$ are computed at the initial condition. Moreover, because the update equations depend only on the inverse matrices via $\alpha_{i \rightarrow \mu}, \alpha_{j \rightarrow \mu}$ or $\mathbf{u}_{i \rightarrow \mu}, \mathbf{v}_{i \rightarrow \mu}$, it is unnecessary to store these matrices in memory. This algorithm, therefore, has a space complexity of $O(|\Omega|R)$. However, it should be noted the Sherman–Morrison formula is prone to high numerical errors compared with standard matrix inversion when λ is close to zero. One must be cautious when employing the algorithm under such condition. Hereafter, we refer to this algorithm as the Gaussian parameterized belief propagation (GPBP) algorithm. The final issue is about a technique for improving the convergence property. For optimal performance, probabilistic damping [12] can be employed in the algorithm, where the factor-to-node messages are updated using the weighted average of the new and old ones. In our algorithm, the damping procedure is given by

$$A_{i \rightarrow \mu}(t+1) = \lambda \mathbf{1}_R + \sum_{v \in \partial i \setminus \mu} \left[(1-\gamma) \frac{\mathbf{v}_{j \rightarrow v}(t) \mathbf{v}_{j \rightarrow v}^\top(t)}{1 + y_{ij}^2 \alpha_{j \rightarrow v}(t)} + \gamma \frac{\mathbf{v}_{j \rightarrow v}(t-1) \mathbf{v}_{j \rightarrow v}^\top(t-1)}{1 + y_{ij}^2 \alpha_{j \rightarrow v}(t-1)} \right], \quad (27)$$

$$\mathbf{B}_{i \rightarrow \mu}(t+1) = \sum_{v \in \partial i \setminus \mu} \left[(1-\gamma) \frac{y_{ij} \mathbf{v}_{j \rightarrow v}(t)}{1 + y_{ij}^2 \alpha_{j \rightarrow v}(t)} + \gamma \frac{y_{ij} \mathbf{v}_{j \rightarrow v}(t-1)}{1 + y_{ij}^2 \alpha_{j \rightarrow v}(t-1)} \right] \quad (28)$$

for $\gamma \in [0, 1]$. Our matrix is still a sum of a diagonal matrix and rank-one matrices, which indicates that the time complexity of the algorithm is nonetheless $O(|\Omega|R^2)$. Note that $A_{i \rightarrow \mu}(t+1)$ and $\mathbf{B}_{i \rightarrow \mu}(t+1)$ are not strictly the weighted sums of $A_{i \rightarrow \mu}(t)$ and $\mathbf{B}_{i \rightarrow \mu}(t)$, but their updated values. In fact, our damping method is equivalent to that in [12] only when γ is sufficiently small. However, at least for the experiments conducted in this study, the employed values provided satisfactory results.

2.2. Approximate BP algorithm

The space complexity of GPBP is $O(|\Omega|R)$, which may be computationally intense when $|\Omega|$ is large. To relax this bottleneck, we apply a common approximation used in deriving approximate message passing (AMP) algorithms from primary BP algorithms [13]. This scheme exploits the fact that each node-to-factor message differs slightly from the sum of the factor-to-node messages when the degree per node is sufficiently large.

Using the Sherman–Morrison formula, the cavity vector at sweep iteration t , $\mathbf{v}_{j \rightarrow \mu}(t)$, is

evaluated as

$$\mathbf{v}_{j \rightarrow \mu}(t) = C_{j \rightarrow \mu}^{-1}(t) \mathbf{D}_{j \rightarrow \mu}(t) \quad (29)$$

$$= \left[C_j^{-1}(t) + \frac{C_j(t)^{-1} \mathbf{u}_{i \rightarrow \mu}(t) \mathbf{u}_{i \rightarrow \mu}^\top(t) C_j^{-1}(t)}{1 + y_{ij}^2 \alpha_{i \rightarrow \mu}(t) - \mathbf{u}_{i \rightarrow \mu}^\top(t) C_j^{-1}(t) \mathbf{u}_{i \rightarrow \mu}(t)} \right] \left[\mathbf{D}_j(t) - \frac{y_{ij} \mathbf{u}_{i \rightarrow \mu}(t)}{1 + y_{ij}^2 \alpha_{i \rightarrow \mu}(t)} \right] \quad (30)$$

$$\simeq \mathbf{v}_j(t) - \frac{y_{ij} - \mathbf{u}_i^\top(t) \mathbf{v}_j(t)}{1 + y_{ij}^2 \alpha_i(t) - \mathbf{u}_i^\top(t) C_j^{-1}(t) \mathbf{u}_i(t)} C_j^{-1}(t) \mathbf{u}_i(t) \equiv \tilde{\mathbf{v}}_{j \rightarrow \mu}(t), \quad (31)$$

where we used the zeroth approximation $\mathbf{u}_{i \rightarrow \mu}(t) \simeq \mathbf{u}_i(t)$ to derive the third line, and $\alpha_i(t) \equiv \mathbf{v}_j^\top(t) C_j^{-1}(t) \mathbf{v}_j(t) / \|\mathbf{v}_j(t)\|^4$. Similarly,

$$C_{j \rightarrow \mu}^{-1}(t) \simeq C_j^{-1}(t) + \frac{C_j^{-1}(t) \mathbf{u}_i(t) \mathbf{u}_i^\top(t) C_j^{-1}(t)}{1 + y_{ij}^2 \alpha_i(t) - \mathbf{u}_i^\top(t) C_j^{-1}(t) \mathbf{u}_i(t)} \equiv \tilde{C}_{j \rightarrow \mu}^{-1}(t), \quad (32)$$

$$\alpha_{j \rightarrow \mu}(t) \simeq \frac{\tilde{\mathbf{v}}_{j \rightarrow \mu}^\top(t) \tilde{C}_{j \rightarrow \mu}^{-1}(t) \tilde{\mathbf{v}}_{j \rightarrow \mu}(t)}{\|\tilde{\mathbf{v}}_{j \rightarrow \mu}(t)\|^4} \equiv \tilde{\alpha}_{j \rightarrow \mu}(t). \quad (33)$$

Substituting (31)–(33) into (24), we obtain the approximated form of $A_i(t+1)$ and $\mathbf{u}_i(t+1)$. Similar update equations are obtained for $C_j(t+1)$ and $\mathbf{v}_j(t+1)$.

It is crucial to correctly evaluate the time dependency of the variables when deriving the approximate algorithms. Although the approximations lead to an iterative algorithm solving a Thouless–Anderson–Palmer-like equation [14] for our system, earlier research [15] showed that intuitive iteration schemes exhibit suboptimal convergence properties. In the above derivation, the time dependencies are completely analogous to GPBP. This approach of mimicking BP was also taken in [15] for compressed sensing, and empirically showed better convergence compared with other methods. To the best of our knowledge, this scheme also gave the best results in our case.

Compared with GPBP, damping has a significant influence on the resultant performance in the approximate algorithm. Approximate probability damping is employed similarly to the case of GPBP by directly damping the node variables using (31) and (33) as

$$A_i(t+1) = \lambda \mathbf{1}_R + \sum_{\mu \in \partial i} \left[(1 - \gamma) \frac{\tilde{\mathbf{v}}_{j \rightarrow \mu}(t) \tilde{\mathbf{v}}_{j \rightarrow \mu}^\top(t)}{1 + y_{ij}^2 \tilde{\alpha}_{j \rightarrow \mu}(t)} + \gamma \frac{\tilde{\mathbf{v}}_{j \rightarrow \mu}(t-1) \tilde{\mathbf{v}}_{j \rightarrow \mu}^\top(t-1)}{1 + y_{ij}^2 \tilde{\alpha}_{j \rightarrow \mu}(t-1)} \right], \quad (34)$$

$$\mathbf{B}_i(t+1) = \sum_{\mu \in \partial i} \left[(1 - \gamma) \frac{y_{ij} \tilde{\mathbf{v}}_{j \rightarrow \mu}(t)}{1 + y_{ij}^2 \tilde{\alpha}_{j \rightarrow \mu}(t)} + \gamma \frac{y_{ij} \tilde{\mathbf{v}}_{j \rightarrow \mu}(t-1)}{1 + y_{ij}^2 \tilde{\alpha}_{j \rightarrow \mu}(t-1)} \right]. \quad (35)$$

Although this implementation requires storing the matrix parameters A_i, C_i explicitly, only the node variables must be kept in memory, which leads to a reduction in the space complexity from $O(|\Omega|R)$ to $O(|\Omega| + (N+M)R^2)$. As $|\Omega| > (N+M)R^2$ must hold for making a matrix recoverable, this reduction in space complexity is beneficial, especially in cases where the number of observations $|\Omega|$ is larger than $N+M$. We refer to this algorithm as the approximated Gaussian parameterized belief propagation (approxGPBP) algorithm.

2.3. Relation to ALS-MP

Unlike GPBP, which handles matrices and vectors, ALS-MP is an iterative algorithm for manipulating only vectors defined on the edges of the factor graphs. However, ALS-MP can be derived from the BP framework with a few modifications from the derivation of GPBP.

Given factor-to-node messages $m_{\mu \rightarrow i}(\mathbf{u}_i)$ and $m_{\mu \rightarrow j}(\mathbf{v}_j)$, we can define *cavity vectors* by maximizing the cavity distributions as

$$\mathbf{u}_{i \rightarrow \mu} = \underset{\mathbf{u}_i}{\operatorname{argmax}} p(\mathbf{u}_i) \prod_{v \in \partial i \setminus \mu} m_{v \rightarrow i}(\mathbf{u}_i), \quad (36)$$

$$\mathbf{v}_{j \rightarrow \mu} = \underset{\mathbf{v}_j}{\operatorname{argmax}} p(\mathbf{v}_j) \prod_{v \in \partial j \setminus \mu} m_{v \rightarrow j}(\mathbf{v}_j). \quad (37)$$

Instead of computing the marginal likelihoods in (7a) and (7c), ALS-MP evaluates factor-to-node messages by inserting the cavity vectors $\mathbf{v}_{j \rightarrow \mu}$ and $\mathbf{u}_{i \rightarrow \mu}$ into the likelihood function as

$$m_{\mu \rightarrow i}(\mathbf{u}_i) \propto p(y_{ij} | \mathbf{u}_i, \mathbf{v}_{j \rightarrow \mu}), \quad (38)$$

$$m_{\mu \rightarrow j}(\mathbf{v}_j) \propto p(y_{ij} | \mathbf{u}_{i \rightarrow \mu}, \mathbf{v}_j). \quad (39)$$

By assigning update indices appropriately, (36)–(39) lead to the following update equations for $\mathbf{u}_{i \rightarrow \mu}$ and $\mathbf{v}_{j \rightarrow \mu}$:

$$\mathbf{u}_{i \rightarrow \mu}(t+1) = \left(\lambda \mathbf{1}_R + \sum_{v \in \partial i \setminus \mu} \mathbf{v}_{j \rightarrow v}(t) \mathbf{v}_{j \rightarrow v}^\top(t) \right)^{-1} \left(\sum_{v \in \partial i \setminus \mu} y_{ij} \mathbf{v}_{j \rightarrow v}(t) \right), \quad (40)$$

$$\mathbf{v}_{j \rightarrow \mu}(t+1) = \left(\lambda \mathbf{1}_R + \sum_{v \in \partial j \setminus \mu} \mathbf{u}_{i \rightarrow v}(t+1) \mathbf{u}_{i \rightarrow v}^\top(t+1) \right)^{-1} \left(\sum_{v \in \partial j \setminus \mu} y_{ij} \mathbf{u}_{i \rightarrow v}(t+1) \right). \quad (41)$$

These are somewhat similar to (19)–(22). Indeed, GPBP is reduced to ALS-MP by dropping all α coefficients. Recall that $\alpha_{i \rightarrow \mu}$ and $\alpha_{j \rightarrow \mu}$ are defined as $\alpha_{i \rightarrow \mu} = \mathbf{v}_{j \rightarrow \mu}^\top C_{j \rightarrow \mu}^{-1} \mathbf{v}_{j \rightarrow \mu} / \|\mathbf{v}_{j \rightarrow \mu}\|^4$ and $\alpha_{j \rightarrow \mu} = \mathbf{u}_{i \rightarrow \mu}^\top A_{i \rightarrow \mu}^{-1} \mathbf{u}_{i \rightarrow \mu} / \|\mathbf{u}_{i \rightarrow \mu}\|^4$. As $C_{j \rightarrow \mu}^{-1}$ and $A_{i \rightarrow \mu}^{-1}$ are proportional to $R \times R$ Fisher information matrices for cavity distributions, this implies that $\alpha_{i \rightarrow \mu}$ and $\alpha_{j \rightarrow \mu}$ play the role of controlling the effect of the observations depending on the uncertainty of the cavity vectors. This property may be beneficial for making estimates robust.

As for its computational aspect, ALS-MP has the same time and space complexity as GPBP, and the same damping techniques can be employed. In addition, its space-saving version, approxALS-MP, can be derived similarly to approxGPBP.

2.4. Performance Evaluation via Population Dynamics

The performance of GPBP and ALS-MP can be evaluated by carrying out experiments for many random instances of the matrices under the given conditions. However, PD [16], which is a sampling method, is more efficient for examining the typical performance of the algorithms in the large system limit of $N, M \rightarrow \infty$. In fact, PD can also be regarded as a method for finding the replica symmetric solution for this system under the framework of the replica theory [16, 17], while applying the approximations which GPBP and ALS-MP adopt.

Interested readers may refer to Appendix B for a derivation of the replica symmetric solution and further discussions about its relation with PD.

We focus on PD for GPBP performed in cases where each row of matrices U and V are linked randomly with c and r observations in Y , respectively, but its generalization to ALS-MP is straightforward. For this, we prepare $N_{\text{PD}} \gg 1$ tuples of $\mathbf{u}^0 \in \mathbb{R}^R$, $\mathbf{u}_{\text{cav}} \in \mathbb{R}^R$, and $\alpha_u \in \mathbb{R}$ for the estimate of U , which are stored in a reservoir that we term “ U -pool.” In addition, their counterparts \mathbf{v}^0 , \mathbf{v}_{cav} , and α_v are also prepared in “ V -pool” for the estimation of V . Here, \mathbf{u}^0 and \mathbf{v}^0 correspond to the transposes of row vectors of the true matrices U^0 and V^0 , whereas \mathbf{u}_{cav} , α_u , \mathbf{v}_{cav} , and α_v represent instances of messages. To update each message tuple in the U -pool, we randomly select $c - 1$ tuples of \mathbf{v}^0 , \mathbf{v}_{cav} , and α_v from the V -pool, and renew \mathbf{u}_{cav} and α_u following the GPBP algorithm handling the $c - 1$ \mathbf{v}_{cav} and α_v as $\mathbf{v}_{j \rightarrow v}$ and $\alpha_{j \rightarrow v}$ and setting $y_{ij} = (\mathbf{u}^0)^\top \mathbf{v}^0 + z$, where z is an independent sample from a certain distribution with zero mean. Similar updates are performed for \mathbf{v}_{cav} and α_v using $r - 1$ tuples of \mathbf{u}^0 , \mathbf{u}_{cav} , and α_u , which are randomly chosen from the U -pool. After iterating these procedures many times, the populations of the message tuples converge to stationary distributions. Then, the estimate of \mathbf{u}^0 is computed by c message tuples chosen randomly from the V -pool, and similarly for \mathbf{v}^0 by r message tuples from the U -pool.

PD simulates the macroscopic behavior of BP when influences of cycles in variable dependence are ignored. The typical lengths of the cycles tend to infinity as $N, M \rightarrow \infty$, and their influences asymptotically vanish when observations in Y are linked randomly with rows of U and V . Therefore, if messages of BP converge to a fixed point, the performance evaluated by the corresponding PD can be regarded as that achieved in the large system limit. However, there is a possibility that the messages will continue to move microscopically, even if their distributions converge macroscopically. In such cases, considerable deviations can be observed between the results of the direct BP experiments and the predictions by PD, which is related to the notion of replica symmetry breaking [13, 18].

3. Numerical Experiments: Synthetic datasets

3.1. Comparison of GPBP and ALS-MP

Synthetic numerical experiments were conducted for both algorithms and their PD counterparts to investigate their performance. The dataset was prepared by generating the original uncorrupted matrix $X \in \mathbb{R}^{N \times M}$ from $U^0 \in \mathbb{R}^{N \times R}$, $V^0 \in \mathbb{R}^{M \times R}$, where the entries of U^0 , V^0 are sampled independently from a standard Gaussian distribution $\mathcal{N}(0, 1)$. Throughout the experiments, the values of M/N and R were fixed to $M/N = 2$ and $R = 10$, where $N = 500$ for both GPBP and ALS-MP, whereas $N_{\text{PD}} = 2000$ for PD experiments. For PD, only the results from a single instance of U^0 and V^0 were obtained because we can expect the self-averaging property to hold.

The observation Y is given by $Y = U^0(V^0)^\top + Z$, where $Z \in \mathbb{R}^{N \times M}$ is a noise matrix. Two types of noise corruptions were considered: Gaussian noise, where the entries of Z are sampled independently from a Gaussian distribution $\mathcal{N}(0, \sigma^2)$ and sparse noise,

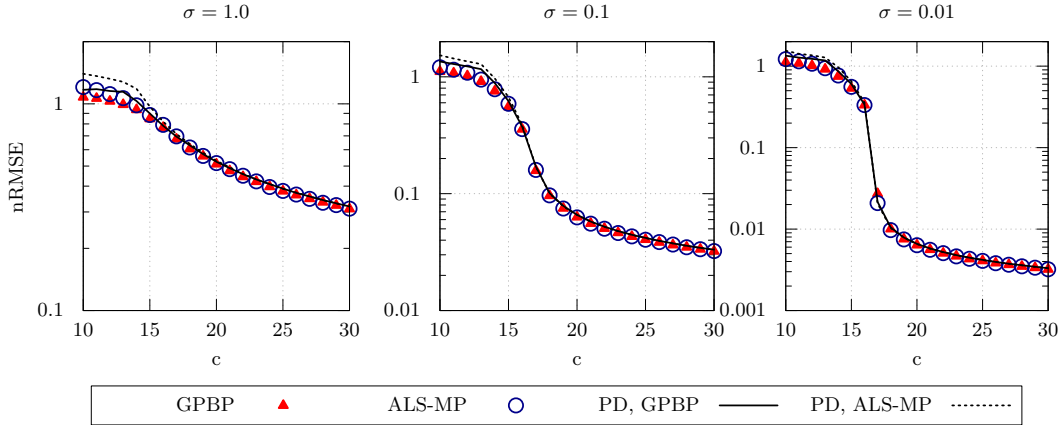


Figure 2. nRMSE of GPBP and ALS-MP for the Gaussian noise case. Throughout the three noise intensities, GPBP and ALS-MP are in agreement when c is above a transitional point. Markers were obtained from the average of 10 random instances.

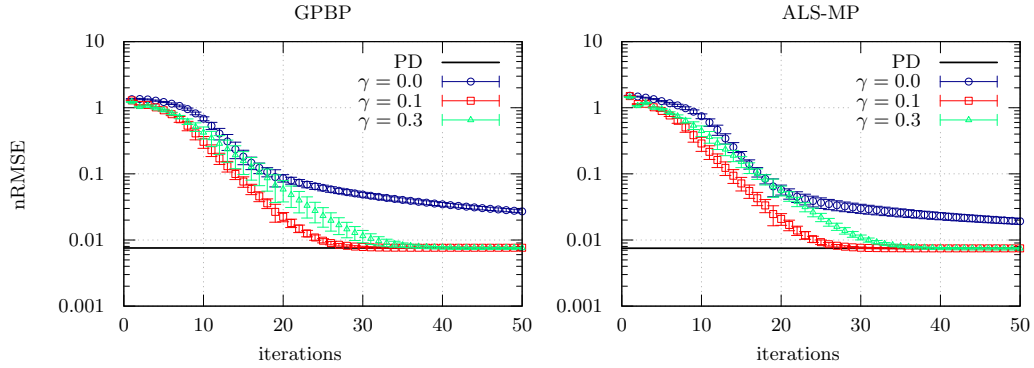


Figure 3. Convergence of GPBP and ALS-MP for $c = 19$ and $\sigma = 0.01$. Both algorithms exhibit a slow convergence to the theoretical prediction given by PD when damping is absent. Markers and error bars represent the averages and standard errors evaluated from 10 random instances.

where the entries of Z are sampled independently from a Bernoulli–Gaussian distribution $0.9\delta(z) + 0.1\mathcal{N}(0, \sigma^2)$. In the Gaussian noise setup, the regularization parameter was set to $\lambda = \sigma^2$, which corresponds to the cases where the problem of (4) intends to maximize the correct posterior distribution composed of (5) and (6). On the other hand, the sparse noise setup represents a situation where the minimization of the squared error $(y_{ij} - \mathbf{u}_i^\top \mathbf{v}_j)^2$ does not match the likelihood maximization, which may be more realistic than the Gaussian noise setup. For both cases, the entries were observed such that each row or column has the same number of observations. Therefore, $c \in \mathbb{N}$ observations were made for each column of matrix Y , whereas $r = cM/N \in \mathbb{N}$ observations were made for each row.

The average performance of GPBP and ALS-MP was evaluated via the normalized RMSE (nRMSE)

$$\text{nRMSE} = \sqrt{(NMR)^{-1} \sum_{i=1}^N \sum_{j=1}^M (x_{ij} - \mathbf{u}_i^\top \mathbf{v}_j)^2}. \quad (42)$$

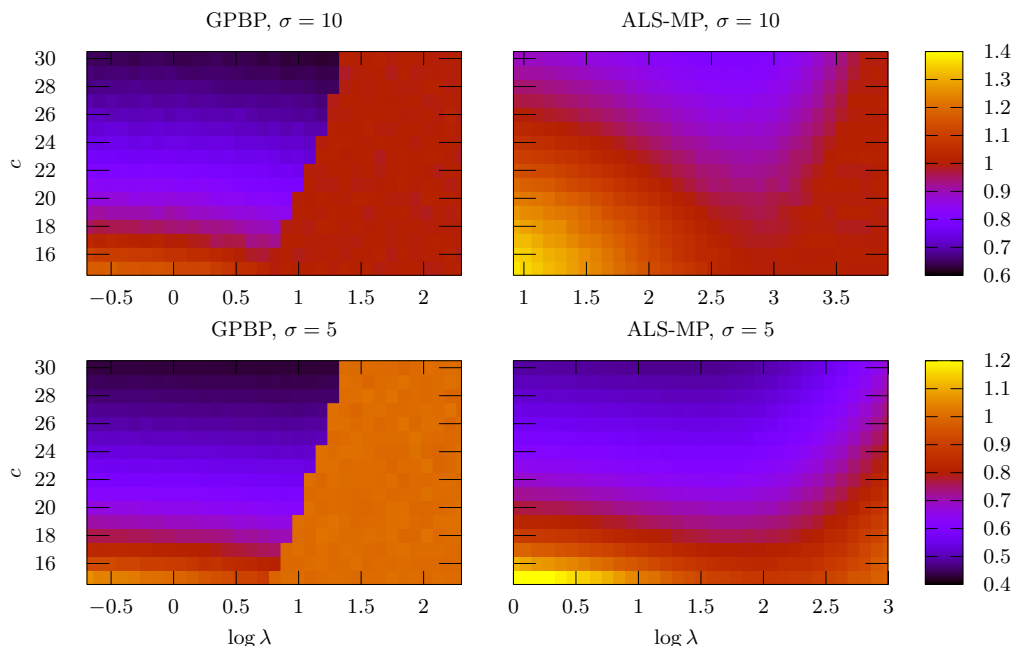


Figure 4. nRMSE of GPBP and ALS-MP assessed by PD. For both $\sigma = 5$ and 10, GPBP achieves a lower nRMSE when λ is set to be optimal for each c . Abrupt performance deterioration occurs for GPBP.

Figure 2 shows nRMSE obtained by GPBP and ALS-MP in the Gaussian noise setup. The behavior of the two algorithms is similar. Differences in the performance, particularly at large values of c and small values of σ , are unclear. It is worth noting that undamped GPBP and ALS-MP cannot achieve the theoretical values predicted by PD, particularly in cases where λ and σ are small. This is evident from figure 3, where the non-damped cases for both GPBP and ALS-MP show worse performance than even the slightly damped case ($\gamma = 0.1$). This indicates that damping is a crucial device for employing BP for the current problem.

The sparse noise setup highlights the difference between GPBP and ALS-MP. Figure 4 shows the nRMSE given by PD for different values of λ . For $\sigma = 5$ and 10, GPBP outperforms ALS-MP at their optimal value of λ . The optimal value of λ for ALS-MP is also significantly larger than that for GPBP, indicating that ALS-MP is more likely to overfit and, hence, is more vulnerable to noise of non-Gaussian types. As stated in Section 2.3, this may be a result of GPBP being able to control the effect of observations more precisely. Figure 5 shows nRMSE given by PD and algorithmic results when λ is fixed near its optimal value. Although deviations between PD and algorithmic results are evident, particularly in large values of σ , overall the two results match fairly well. Interestingly, the qualitative behavior of GPBP and ALS-MP differs greatly with respect to different values of λ . Although an abrupt performance deterioration occurs for GPBP above a certain value of λ , where the solution discontinuously shrinks to $U = 0, V = 0$, the nRMSE of ALS-MP varies smoothly. This implies the possibility that GPBP exhibits a discontinuous phase transition, whereas that of ALS-MP is continuous.

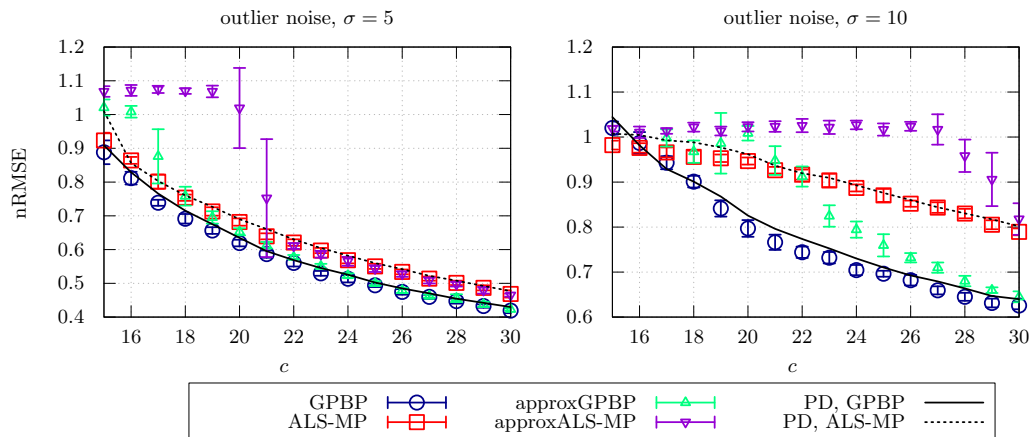


Figure 5. nRMSE of GBP, ALS-MP, approxGBP, and approxALS-MP near the optimal value of λ ($\lambda_{\text{GBP}} = 1.85, \lambda_{\text{ALS-MP}} = 4.91$ for $\sigma = 5$, and $\lambda_{\text{GBP}} = 1.85, \lambda_{\text{ALS-MP}} = 14.8$ for $\sigma = 10$). Markers and error bars represent averages and standard errors evaluated from 10 random instances.

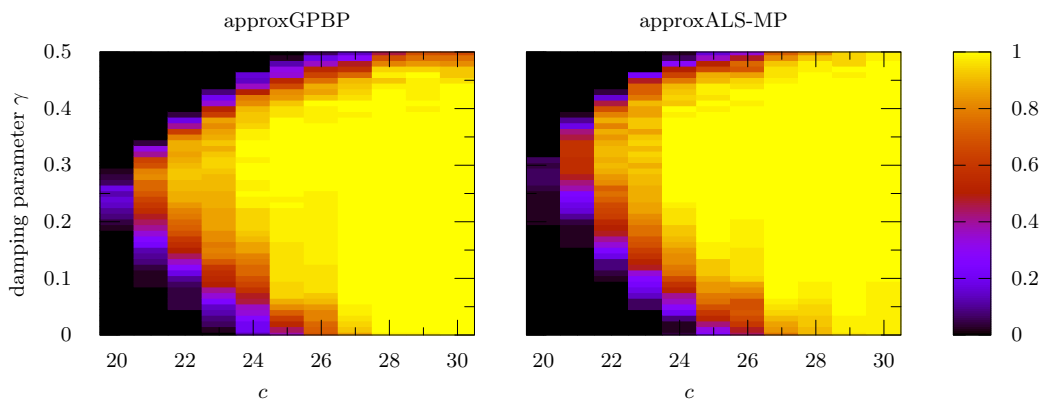


Figure 6. Reconstruction rate of approxGBP and approxALS-MP for $\sigma = \epsilon = 0.01$ obtained from 100 random instances under different damping parameters. Both algorithms can reconstruct the matrix from $c \sim 22$ under appropriate damping.

3.2. Comparison of approxGBP and approxALS-MP

Damping plays a more significant role to achieve optimal performance for approxGBP and approxALS-MP. In fact, both approximation algorithms sometimes cease to converge when c is small. Therefore, we evaluate the performance of the algorithms by reconstruction rate, defined by the empirical probability of nRMSE being lower than some threshold value ϵ .

Figure 6 shows the reconstruction rate of approxGBP and approxALS-MP for Gaussian noise with $\sigma = \epsilon = 0.01$ for different damping parameters. Tuning the damping parameters appropriately significantly improves the reconstruction quality; the reconstruction threshold can be reduced from $c \sim 26$ to $c \sim 22$, when damping is optimal. Quantitatively, similar results were obtained for different values of σ and ϵ . Both algorithms exhibit similar performance (in terms of the threshold and nRMSE) in the Gaussian noise setup, which is consistent with the results obtained for the non-approximated counterparts.

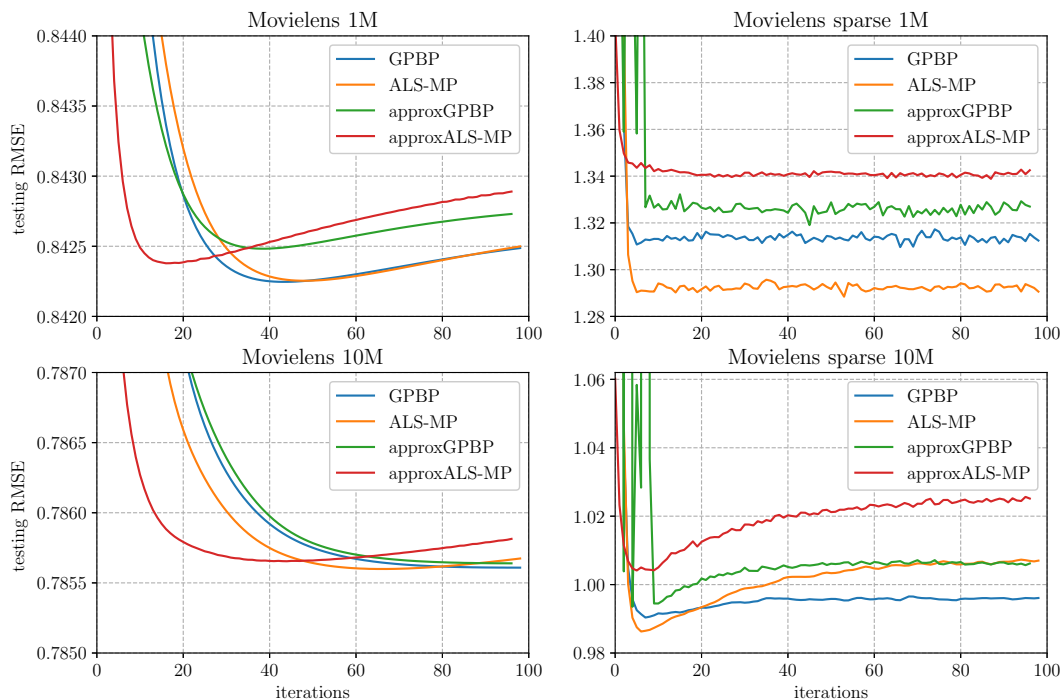


Figure 7. RMSE of the four algorithms for the (sparse) 1M and (sparse) 10M dataset. The RMSE was obtained from the average of a 10-fold cross-validation.

Consistency with the results from the non-approximated algorithms is also evident in the sparse noise setup in figure 5, where approxGPBP outperforms approxALS-MP in both noise intensities. The performance of approxGPBP and approxALS-MP seems to encounter a transition from an uninformative to informative phase, with a margin where approxGPBP can obtain information on the matrix ($n\text{RMSE} < 1$), whereas approxALS-MP cannot. We speculate that this is another benefit gained by employing more informative messages in GPBP/approxGPBP. Nevertheless, as c increases, the performance of approxGPBP and approxALS-MP asymptotically approaches that of the non-approximated versions, indicating that our perturbation treatment is valid.

4. Numerical Experiments: Real-world Datasets

The performance of the algorithms in practical settings was evaluated via application to the 1M and 10M Movielens datasets [19], which are commonly used benchmark datasets for recommender systems. The 1M (10M) dataset consists of 1000209 (10000054) discrete ratings given by 6040 (69878) users on 3952 (10677) movies. All users are guaranteed to have rated at least 20 movies. The average number of ratings per user/movie is $c \sim 100$, which may make the task relatively easy owing to its dense connection. Therefore, a sparsified version of 1M and 10M Movielens datasets, which only takes into account users who gave less than 31 ratings, was used as the benchmark. This subset, denoted as the sparse 1M (10M) Movielens dataset, has 18169 (295831) ratings given by 750 (12343) users on 2356 (6484) movies.

We evaluated the algorithm’s performance based on a 10-fold nested cross-validation procedure; each dataset was split into 10 random subsets of equal size, and 9 out of 10 subsets were used for training, while the remaining dataset was used to assess the RMSE. Five percent of the training dataset was held out as a validation dataset to determine the value of λ , while the remaining 95% was used for training. The average of the 10 RMSE values was reported as the final RMSE score. The rank of the matrix U, V was set to $R = 10$. The regularization parameter was chosen from 11 geometrically spaced values in the range $[1, 5]$ for 1M, sparse 1M, and sparse 10M datasets, and 6 geometrically spaced values in range $[1, 5]$ for the 10M dataset.

Results from the above procedure on the four datasets are given in figure 7. As speculated, GPBP and ALS-MP exhibit little difference in performance on the relatively dense 1M dataset. The 10M dataset shows a similar trend, although ALS-MP converges faster than GPBP. However, ALS-MP presents signs of overfitting, where the test RMSE increases after achieving a minimum value. Mixed results are obtained for sparse datasets. Although dominant for the sparse 1M dataset, ALS-MP strongly overfits the training data for the sparse 10M dataset. Consistently, approxGPBP outperforms approxALS-MP for all four datasets, suggesting that our Gaussian treatment of messages is also beneficial for handling real-world data with low space complexity.

5. Conclusion

In this study, we developed a Gaussian-based BP algorithm, GPBP, for the noisy matrix completion problem. By factorizing the inferred matrix and parameterizing the cavity distributions as Gaussians, the problem of continuous degrees of freedom in message passing was reduced to that of only a few variables. The relation to a similar message-passing algorithm, ALS-MP, developed in the literature, was discussed. In addition, approximate but memory-friendly versions of GPBP and ALS-MP, namely approxGPBP and approxALS-MP, respectively, were derived by a perturbation treatment.

Experiments on synthetic data with Gaussian noise indicated that there is little to no difference in performance between GPBP and ALS-MP. In contrast, those with non-Gaussian noise showed that GPBP can exhibit better performance compared with ALS-MP. A similar result was also obtained for their approximate counterparts, approxGPBP and approxALS-MP.

Experiments on the Movielens datasets indicated that GPBP and ALS-MP provide similar performance, but GPBP is more robust against overfitting under fewer data. The experiments also showed that approxGPBP exhibits better performance than approxALS-MP for the datasets. This implies that for larger datasets where space complexity is an issue, approxGPBP could be a better choice.

It is important to emphasize that although the Gaussian approximation of the posterior distribution empirically offered good performance, theoretically, this is suboptimal. This is because the matrix factorization model belongs to a family of singular statistical models [20], where the posterior distribution is generally approximated poorly by a Gaussian distribution

even when many data are employed. It is important to examine the effect of singularity on factorized Gaussian approximations, and whether further improvements can be performed by a more legitimate parameterization.

Although our approach is based on nuclear norm minimization, several recent studies (for example, [21]) achieved a lower error in real-world datasets in more complex problem settings. However, our method can still be advantageous in terms of time or space complexity owing to its simplicity. Incorporating our method in novel algorithms to reduce computational costs is another future research direction.

Acknowledgments

The authors would like to thank Takashi Takahashi and Masato Okada for helpful insights. This work was partially funded by JSPS KAKENHI No. 17H00764 and JST CREST Grant Number JPMJCR1912, Japan (YK).

Appendix A. Derivation of equation (11)

Herein, we derive (11). Dropping all indices and substituting (5) and (10b) into (7a), we obtain

$$\begin{aligned} m_{\mu \rightarrow i}(\mathbf{u}) &\propto \int d\mathbf{v} \exp \left[-\frac{\beta}{2} (y - \mathbf{u}^\top \mathbf{v})^2 - \frac{\beta}{2} \mathbf{v}^\top C \mathbf{v} + \beta \mathbf{D}^\top \mathbf{v} \right] \\ &= |C + \mathbf{u}\mathbf{u}^\top|^{-1/2} \exp \left[\frac{\beta}{2} (\mathbf{D} + y\mathbf{u})^\top (C + \mathbf{u}\mathbf{u}^\top)^{-1} (\mathbf{D} + y\mathbf{u}) \right]. \end{aligned} \quad (\text{A.1})$$

The term in the exponential in (A.1) is manipulated using the Sherman–Morrison formula:

$$\begin{aligned} \frac{1}{2} (\mathbf{D} + y\mathbf{u})^\top (C + \mathbf{u}\mathbf{u}^\top)^{-1} (\mathbf{D} + y\mathbf{u}) &= \frac{1}{2} (\mathbf{D} + y\mathbf{u})^\top \left(C^{-1} - \frac{C^{-1} \mathbf{u}\mathbf{u}^\top C^{-1}}{1 + \mathbf{u}^\top C^{-1} \mathbf{u}} \right) (\mathbf{D} + y\mathbf{u}) \\ &= \frac{y^2}{2} \frac{\mathbf{u}^\top C^{-1} \mathbf{u}}{1 + \mathbf{u}^\top C^{-1} \mathbf{u}} - \frac{1}{2} \frac{(\mathbf{u}^\top C^{-1} \mathbf{D})^2}{1 + \mathbf{u}^\top C^{-1} \mathbf{u}} + y \frac{\mathbf{u}^\top C^{-1} \mathbf{D}}{1 + \mathbf{u}^\top C^{-1} \mathbf{u}} + \text{Const.}, \end{aligned} \quad (\text{A.2})$$

where Const. represents the terms that are independent of \mathbf{u} . Note that since $\mathbf{u}^\top C^{-1} \mathbf{u} / (1 + \mathbf{u}^\top C^{-1} \mathbf{u}) = 1 - 1/(1 + \mathbf{u}^\top C^{-1} \mathbf{u})$ in the first term, (A.2) is given by

$$-\frac{1}{2} \frac{(y - \mathbf{u}^\top C^{-1} \mathbf{D})^2}{1 + \mathbf{u}^\top C^{-1} \mathbf{u}} + \text{Const.} \quad (\text{A.3})$$

Using (A.3) and the matrix determinant lemma $|C + \mathbf{u}\mathbf{u}^\top| = |C|(1 + \mathbf{u}^\top C^{-1} \mathbf{u})$ in (A.1), we obtain (11).

Appendix B. Replica computation and its relation to population dynamics

Handling the objective function of (4) as the Hamiltonian, the partition function is computed as:

$$Z_\beta(L, U^0, V^0) = \int dU dV \exp \left[-\frac{\beta}{2} \sum_{i,j} L_{ij} (\mathbf{u}_i^\top \mathbf{v}_j - (\mathbf{u}_i^0)^\top \mathbf{v}_j^0)^2 - \frac{\beta\lambda}{2} \sum_{i=1}^N \|\mathbf{u}_i\|^2 - \frac{\beta\lambda}{2} \sum_{j=1}^M \|\mathbf{v}_j\|^2 \right], \quad (\text{B.1})$$

where $L = \{L_{ij}\} \in \{0, 1\}^{N \times M}$ is a sparse binary matrix, and $U^0 = (\mathbf{u}_1^0, \dots, \mathbf{u}_N^0)^\top$, $V^0 = (\mathbf{v}_1^0, \dots, \mathbf{v}_M^0)^\top$ is the ground truth (planted) matrix. In particular, we are interested in the free energy at zero temperature $\phi = \lim_{\beta \rightarrow \infty} \lim_{N, M \rightarrow \infty} (N\beta)^{-1} \log Z_\beta$, as this enables us to assess the macroscopic properties of the maximum of the posterior distribution specified by (5) and (6). Here, the limit of $N, M \rightarrow \infty$ is taken such that the ratio $\alpha \equiv M/N$ is kept constant. The free energy ϕ is a random variable depending on the configuration of random variables L and U^0, V^0 . The configurational average of ϕ , often referred to as the *quenched* average, can be calculated using the replica method, which is based on the following identity:

$$\langle \log Z_\beta \rangle_{L, U^0, V^0} = \lim_{n \rightarrow +0} \frac{1}{n} \log \langle Z_\beta^n \rangle_{L, U^0, V^0}, \quad (\text{B.2})$$

where $\langle \dots \rangle_{L, U^0, V^0}$ stands for the configurational average with respect to L, U^0 , and V^0 . To avoid the difficulty of calculating $\langle Z_\beta^n \rangle_{L, U^0, V^0}$ for $n \in \mathbb{R}$, the configurational average of Z_β^n is first calculated as an analytic form of $n \in \mathbb{N}$, and the limit of $n \rightarrow +0$ is taken via analytical continuation to $n \in \mathbb{R}$.

Herein, we derive the replica symmetric solution along the lines of [22] and [23]. While we consider only the case where L is a matrix with c nonzero matrix elements per column and r nonzero elements per row (so $Nr = Mc$), generalization to other binary masks is straightforward. The planted matrices U^0, V^0 are assumed to follow the distribution $p_U^0(U^0) = \prod_{i=1}^N p_U^0(\mathbf{u}_i^0)$, $p_V^0(V^0) = \prod_{j=1}^M p_V^0(\mathbf{v}_j^0)$. First, the average over all configurations of L is given by

$$\begin{aligned} \langle (\dots) \rangle_L &= \mathcal{N}^{-1} \text{Tr}_L (\dots) \delta \left(\sum_i L_{ij}, c \right) \delta \left(\sum_j L_{ij}, r \right) \\ &= \mathcal{N}^{-1} \prod_{i=1}^N \left(\oint \frac{dz_i}{2\pi\sqrt{-1}} z_i^{c+1} \right) \prod_{j=1}^M \left(\oint \frac{dw_j}{2\pi\sqrt{-1}} w_j^{r+1} \right) \text{Tr}_L (\dots) (z_i w_j)^{L_{ij}}, \end{aligned} \quad (\text{B.3})$$

Where we used the integral representation of the Kronecker delta. Here, $\text{Tr}_L = \prod_{i,j} \sum_{L_{ij}=0,1}$, and \mathcal{N} is the total number of configurations, which can be calculated using the saddle point method as [22]

$$\mathcal{N} = \exp(Nr \log Nr - Nr - N \log r! - M \log c!).$$

Taking the n -replicated partition function indexed by $a = 1, \dots, n$, and averaging over L, U^0 , and V^0 offers

$$\begin{aligned} \langle Z_\beta^n \rangle_{C, U^0, V^0} &= \mathcal{N}^{-1} \prod_{i=1}^N \left(\oint \frac{dz_i}{2\pi\sqrt{-1}} z_i^{c+1} \right) \prod_{j=1}^M \left(\oint \frac{dw_j}{2\pi\sqrt{-1}} w_j^{r+1} \right) \int \prod_{a=0}^n dU^a dV^a p_U^0(U^0) p_V^0(V^0) \\ &\quad \times \text{Tr}_L \prod_{i,j} \left\{ (z_i w_j)^{L_{ij}} \exp \left[-\frac{\beta}{2} \sum_{i,j} L_{ij} \sum_{a=1}^n ((\mathbf{u}_i^a)^\top \mathbf{v}_j^a - (\mathbf{u}_i^0)^\top \mathbf{v}_j^0)^2 - \frac{\beta\lambda}{2} \sum_{a,i} \|\mathbf{u}_i^a\|^2 - \frac{\beta\lambda}{2} \sum_{a,j} \|\mathbf{v}_j^a\|^2 \right] \right\}. \end{aligned} \quad (\text{B.4})$$

The summation over L_{ij} can be evaluated as

$$\begin{aligned}
& \text{Tr} \prod_{i,j} \left\{ (z_i w_j)^{L_{ij}} \exp \left[-\frac{\beta}{2} \sum_{i,j} L_{ij} \sum_{a=1}^n ((\mathbf{u}_i^a)^\top \mathbf{v}_j^a - (\mathbf{u}_i^0)^\top \mathbf{v}_j^0)^2 \right] \right\} \\
&= \prod_{i,j} \left\{ 1 + z_i w_j \exp \left[-\frac{\beta}{2} \sum_{a=1}^n ((\mathbf{u}_i^a)^\top \mathbf{v}_j^a - (\mathbf{u}_i^0)^\top \mathbf{v}_j^0)^2 \right] \right\} \\
&= \exp \left\{ \sum_{i,j} \log \left[1 + z_i w_j \exp \left[-\frac{\beta}{2} \sum_{a=1}^n ((\mathbf{u}_i^a)^\top \mathbf{v}_j^a - (\mathbf{u}_i^0)^\top \mathbf{v}_j^0)^2 \right] \right] \right\} \\
&\simeq \exp \left\{ \sum_{i,j} z_i w_j \exp \left[-\frac{\beta}{2} \sum_{a=1}^n ((\mathbf{u}_i^a)^\top \mathbf{v}_j^a - (\mathbf{u}_i^0)^\top \mathbf{v}_j^0)^2 \right] \right\}. \tag{B.5}
\end{aligned}$$

Now, define order parameter functions as

$$Q(\{\mathbf{u}^a\}) = \frac{1}{N} \sum_{i=1}^N z_i \prod_{a=0}^n \delta(\mathbf{u}_i^a - \mathbf{u}^a), \quad q(\{\mathbf{v}^a\}) = \frac{1}{M} \sum_{j=1}^M w_j \prod_{a=0}^n \delta(\mathbf{v}_j^a - \mathbf{v}^a), \tag{B.6}$$

and their conjugate functions, denoted by \hat{Q}, \hat{q} , to constrain Q, q to obey the above relations. More explicitly, we use the equality

$$\begin{aligned}
1 &= \int [DQ] \delta \left(\frac{1}{N} \sum_{i=1}^N z_i \prod_{a=0}^n \delta(\mathbf{u}_i^a - \mathbf{u}^a) - Q(\{\mathbf{u}^a\}) \right) \\
&= \int [DQ][D\hat{Q}] \exp \left[- \int d\{\mathbf{u}^a\} N Q(\{\mathbf{u}^a\}) \hat{Q}(\{\mathbf{u}^a\}) + \int d\{\mathbf{u}^a\} \hat{Q}(\{\mathbf{u}^a\}) \sum_{i=1}^N z_i \prod_{a=0}^n \delta(\mathbf{u}_i^a - \mathbf{u}^a) \right], \tag{B.7}
\end{aligned}$$

and

$$\begin{aligned}
1 &= \int [Dq] \delta \left(\frac{1}{M} \sum_{j=1}^M w_j \prod_{a=0}^n \delta(\mathbf{v}_j^a - \mathbf{v}^a) - q(\{\mathbf{v}^a\}) \right) \\
&= \int [Dq][D\hat{q}] \exp \left[- \int d\{\mathbf{v}^a\} M q(\{\mathbf{v}^a\}) \hat{q}(\{\mathbf{v}^a\}) + \int d\{\mathbf{v}^a\} \hat{q}(\{\mathbf{v}^a\}) \sum_{j=1}^M w_j \prod_{a=0}^n \delta(\mathbf{v}_j^a - \mathbf{v}^a) \right], \tag{B.8}
\end{aligned}$$

which is verified by employing results from functional integration. Using (B.6), (B.5) is expressed as

$$\begin{aligned}
& \sum_{i,j} z_i w_j \exp \left\{ -\frac{\beta}{2} \sum_{a=1}^n ((\mathbf{u}_i^a)^\top \mathbf{v}_j^a - (\mathbf{u}_i^0)^\top \mathbf{v}_j^0)^2 \right\} \\
&= NM \int d\{\mathbf{u}^a\} d\{\mathbf{v}^a\} Q(\{\mathbf{u}^a\}) q(\{\mathbf{v}^a\}) \exp \left[-\frac{\beta}{2} \sum_{a=1}^n ((\mathbf{u}^a)^\top \mathbf{v}^a - (\mathbf{u}^0)^\top \mathbf{v}^0)^2 \right]. \tag{B.9}
\end{aligned}$$

Inserting equality (B.7) and (B.8), and using (B.5) and (B.9) to (B.4), the integral over z_i and w_j can be performed. Employing the saddle point method with respect to the order parameter functions Q, q, \hat{Q} , and \hat{q} offers the logarithm of the configurational average of Z_β^n :

$$\begin{aligned} \frac{1}{N} \log \langle Z_\beta^n \rangle_{C, U^0, V^0} &= \text{Extr}_{Q, q, \hat{Q}, \hat{q}} \left\{ M \int d\{\mathbf{u}^a\} d\{\mathbf{v}^a\} Q(\{\mathbf{u}^a\}) q(\{\mathbf{v}^a\}) \exp \left[-\frac{\beta}{2} \sum_{a=1}^n ((\mathbf{u}^a)^\top \mathbf{v}^a - (\mathbf{u}^0)^\top \mathbf{v}^0)^2 \right] \right. \\ &\quad - \int d\{\mathbf{u}^a\} Q(\{\mathbf{u}^a\}) \hat{Q}(\{\mathbf{u}^a\}) - \alpha \int d\{\mathbf{v}^a\} q(\{\mathbf{v}^a\}) \hat{q}(\{\mathbf{v}^a\}) \\ &\quad + \log \int d\{\mathbf{u}^a\} p_U^0(\mathbf{u}^0) \hat{Q}^c(\{\mathbf{u}^a\}) \exp \left(-\frac{\beta\lambda}{2} \sum_{a=1}^n \|\mathbf{u}^a\|^2 \right) \\ &\quad \left. + \alpha \log \int d\{\mathbf{v}^a\} p_V^0(\mathbf{v}^0) \hat{q}^r(\{\mathbf{v}^a\}) \exp \left(-\frac{\beta\lambda}{2} \sum_{a=1}^n \|\mathbf{v}^a\|^2 \right) - r \log(Nr) + r \right\}. \end{aligned} \quad (\text{B.10})$$

Now, we assume that the saddle point is dominated by the order parameter functions of the form

$$Q(\{\mathbf{u}^a\}) = P_U(\mathbf{u}^0) \int [Df] \rho_U(f|\mathbf{u}^0) \prod_{a=1}^n \frac{e^{-\beta f(\mathbf{u}^a)}}{\int d\mathbf{u} e^{-\beta f(\mathbf{u})}}, \quad (\text{B.11})$$

$$q(\{\mathbf{v}^a\}) = P_V(\mathbf{v}^0) \int [Dg] \rho_V(g|\mathbf{v}^0) \prod_{a=1}^n \frac{e^{-\beta g(\mathbf{v}^a)}}{\int d\mathbf{v} e^{-\beta g(\mathbf{v})}}, \quad (\text{B.12})$$

$$\hat{Q}(\{\mathbf{u}^a\}) = \hat{P}_U(\mathbf{u}^0) \int [D\hat{f}] \hat{\rho}_U(\hat{f}|\mathbf{u}^0) \exp \left(-\beta \sum_{a=1}^n \hat{f}(\mathbf{u}^a) \right), \quad (\text{B.13})$$

$$\hat{q}(\{\mathbf{v}^a\}) = \hat{P}_V(\mathbf{v}^0) \int [D\hat{g}] \hat{\rho}_V(\hat{g}|\mathbf{v}^0) \exp \left(-\beta \sum_{a=1}^n \hat{g}(\mathbf{v}^a) \right). \quad (\text{B.14})$$

Here, functionals $\rho_U, \rho_V, \hat{\rho}_U$, and $\hat{\rho}_V$ are distributions of functions, and P_U, P_V, \hat{P}_U , and \hat{P}_V are potentially non-normalized functions. This form of order parameter functions is induced from the replica symmetric ansatz [17], where Q, q, \hat{Q} , and \hat{q} are functions symmetric with respect to permutations of replica indices $a = 1, \dots, n$. Inserting these expressions to (B.10), and extremizing with respect to functions P_U, P_V, \hat{P}_U , and \hat{P}_V in the limit $n \rightarrow 0$ offers

$$\hat{P}_U \hat{P}_V = Nc, \quad P_U(\mathbf{u}^0) \hat{P}_U = c p_U^0(\mathbf{u}^0), \quad P_V(\mathbf{v}^0) \hat{P}_V = r p_V^0(\mathbf{v}^0). \quad (\text{B.15})$$

Using (B.15) and the Laplace method to evaluate the integrals in the limit $\beta \rightarrow \infty$ for (B.10), we obtain the free energy as

$$\begin{aligned} \frac{\phi}{c} &= \lim_{\beta \rightarrow \infty} \frac{1}{\beta} \lim_{N \rightarrow \infty} \lim_{n \rightarrow +0} \frac{1}{nNc} \log \langle Z^n(\beta, C) \rangle_{C, U^0, V^0} \\ &= \text{Extr}_{\rho_U, \rho_V, \hat{\rho}_U, \hat{\rho}_V} \left\{ - \left\langle \min_{\mathbf{u}, \mathbf{v}} \left[\frac{1}{2} (\mathbf{u}^\top \mathbf{v} + (\mathbf{u}^0)^\top \mathbf{v}^0)^2 + f(\mathbf{u}) + g(\mathbf{v}) \right] - \min_{\mathbf{u}} f(\mathbf{u}) - \min_{\mathbf{v}} g(\mathbf{v}) \right\rangle_{\mathbf{u}^0, \mathbf{v}^0, f, g} \right. \\ &\quad + \left\langle \min_{\mathbf{u}} (f(\mathbf{u}) + \hat{f}(\mathbf{u})) - \min_{\mathbf{u}} f(\mathbf{u}) \right\rangle_{\mathbf{u}^0, f, \hat{f}} + \left\langle \min_{\mathbf{v}} (g(\mathbf{v}) + \hat{g}(\mathbf{v})) - \min_{\mathbf{v}} g(\mathbf{v}) \right\rangle_{\mathbf{v}^0, g, \hat{g}} \\ &\quad \left. - \frac{1}{c} \left\langle \min_{\mathbf{u}} \left[\frac{\lambda}{2} \|\mathbf{u}\|^2 + \sum_{k=1}^c \hat{f}_k(\mathbf{u}) \right] \right\rangle_{\mathbf{u}^0, \{\hat{f}_k\}_{k=1}^c} - \frac{1}{r} \left\langle \min_{\mathbf{v}} \left[\frac{\lambda}{2} \|\mathbf{v}\|^2 + \sum_{l=1}^r \hat{g}_l(\mathbf{v}) \right] \right\rangle_{\mathbf{v}^0, \{\hat{g}_l\}_{l=1}^r} \right\}. \quad (\text{B.16}) \end{aligned}$$

where $\langle \cdots \rangle_{\mathbf{u}^0, \mathbf{v}^0, f, g}$ represents the average operation with respect to $p_U^0(\mathbf{u}^0)$, $p_V^0(\mathbf{v}^0)$, $\rho(f|\mathbf{u}^0)$, $\rho(g|\mathbf{v}^0)$, and similarly for the other brackets. By taking the function derivative with respect to $\rho_U, \rho_V, \hat{\rho}_U, \hat{\rho}_V$, it can be confirmed that the equations of state which describe the replica symmetric solution are given by the following:

$$\hat{\rho}_U(\hat{f}|\mathbf{u}^0) = \left\langle \delta \left(\hat{f}(\mathbf{u}) - \min_{\mathbf{v}} \left[\frac{1}{2} (\mathbf{u}^\top \mathbf{v} - (\mathbf{u}^0)^\top \mathbf{v}^0)^2 + g(\mathbf{v}) \right] + \min_{\mathbf{v}} g(\mathbf{v}) \right) \right\rangle_{\mathbf{v}^0, g}, \quad (\text{B.17})$$

$$\hat{\rho}_V(\hat{g}|\mathbf{v}^0) = \left\langle \delta \left(\hat{g}(\mathbf{v}) - \min_{\mathbf{u}} \left[\frac{1}{2} (\mathbf{u}^\top \mathbf{v} - (\mathbf{u}^0)^\top \mathbf{v}^0)^2 + f(\mathbf{u}) \right] + \min_{\mathbf{u}} f(\mathbf{u}) \right) \right\rangle_{\mathbf{u}^0, f}, \quad (\text{B.18})$$

$$\rho_U(f|\mathbf{u}^0) = \left\langle \delta \left(f(\mathbf{u}) - \sum_{k=1}^{c-1} \hat{f}_k(\mathbf{u}) - \frac{\lambda}{2} \|\mathbf{u}\|^2 \right) \right\rangle_{\mathbf{v}^0, \{\hat{f}_k\}_{k=1}^{c-1}}, \quad (\text{B.19})$$

$$\rho_V(g|\mathbf{v}^0) = \left\langle \delta \left(g(\mathbf{v}) - \sum_{l=1}^{r-1} \hat{g}_l(\mathbf{v}) - \frac{\lambda}{2} \|\mathbf{v}\|^2 \right) \right\rangle_{\mathbf{u}^0, \{\hat{g}_l\}_{l=1}^{r-1}}. \quad (\text{B.20})$$

These can easily be augmented to the noisy case by adding a noise term to $(\mathbf{u}^0)^\top \mathbf{v}^0$ and averaging over its distribution in (B.17) and (B.18).

The system of equations (B.17)–(B.20) determine the probability density of functions f, g, \hat{f} and \hat{g} , which correspond to cavity biases and cavity distributions in the BP algorithm. Thus, the replica symmetric solution describes, by nature, the typical properties of cavity biases and cavity distributions in the form of its distribution on functional space. PD aims to solve this set of equations by preparing a population of f, g, \mathbf{u}^0 and \mathbf{v}^0 , and performing Monte Carlo sampling for (B.17)–(B.20). The empirical distribution of f and g obtained from the population after sufficient sampling iterations approximates the fixed point of the equations of state in the large population size limit [16]. Again, the problem of continuous degrees of freedom persists; this is avoided by approximating the functions by a Gaussian, which reduces to the PD algorithm in 2.4.

References

- [1] Hastie T, Tibshirani R and Wainwright M 2015 *Statistical Learning with Sparsity: The Lasso and Generalizations* (Boca Raton, FL: Chapman & Hall/CRC)

- [2] Candes E J and Plan Y 2010 *Proceedings of the IEEE* **98** 925–936
- [3] Keshavan R H, Montanari A and Oh S 2010 *Journal of Machine Learning Research* **11** 2057–2078
- [4] Koltchinskii V, Lounici K and Tsybakov A B 2011 *The Annals of Statistics* **39**
- [5] Ge R, Lee J D and Ma T 2016 *Advances in Neural Information Processing Systems* **29** 2973–2981
- [6] Keshavan R H 2012 *Efficient algorithms for collaborative filtering* Ph.D. thesis Stanford University
- [7] Gamarnik D and Misra S 2016 *IEEE Signal Processing Letters* **23** 1340–1343
- [8] Noguchi C and Kabashima Y 2019 *Journal of Physics A: Mathematical and Theoretical* **52** 424004
- [9] Jain P, Netrapalli P and Sanghavi S 2013 Low-rank matrix completion using alternating minimization *Proceedings of the Forty-Fifth Annual ACM Symposium on Theory of Computing* (New York, NY, USA: Association for Computing Machinery) p 665–674
- [10] Minka T P 2001 Expectation propagation for approximate bayesian inference *Proceedings of the Seventeenth Conference on Uncertainty in Artificial Intelligence* (San Francisco, CA, USA: Morgan Kaufmann Publishers Inc.) p 362–369
- [11] Recht B, Fazel M and Parrilo P A 2010 *SIAM Rev.* **52** 471–501
- [12] Pretti M 2005 *Journal of Statistical Mechanics: Theory and Experiment* **2005** P11008–P11008
- [13] Kabashima Y 2003 *Journal of Physics A: Mathematical and General* **36** 11111–11121
- [14] Thouless D J, Anderson P W and Palmer R G 1977 *The Philosophical Magazine: A Journal of Theoretical Experimental and Applied Physics* **35** 593–601
- [15] Manoel A, Krzakala F, Tramel E and Zdeborová L 2015 Swept approximate message passing for sparse estimation *Proceedings of the 32nd International Conference on Machine Learning (Proceedings of Machine Learning Research vol 37)* (PMLR) pp 1123–1132
- [16] Mezard M and Montanari A 2009 *Information, Physics, and Computation* (USA: Oxford University Press, Inc.) ISBN 019857083X
- [17] Nishimori H 2001 *Statistical Physics of Spin Glasses and Information Processing: an Introduction* (Oxford: Oxford University Press)
- [18] Takahashi T and Kabashima Y 2020 Macroscopic analysis of vector approximate message passing in a model mismatch setting *2020 IEEE International Symposium on Information Theory (ISIT)* pp 1403–1408
- [19] Harper F M and Konstan J A 2015 *ACM Trans. Interact. Intell. Syst.* **5** 19:1–19:19
- [20] Watanabe S 2001 *Neural Networks* **14** 1049–1060
- [21] Salakhutdinov R and Mnih A 2008 Bayesian probabilistic matrix factorization using markov chain monte carlo *Proceedings of the 25th International Conference on Machine Learning* (New York, NY, USA: Association for Computing Machinery) pp 880–887
- [22] Murayama T, Kabashima Y, Saad D and Vicente R 2000 *Phys. Rev. E* **62**(2) 1577–1591
- [23] Kabashima Y and Takahashi H 2012 *Journal of Physics A: Mathematical and Theoretical* **45** 325001